The stimulation of grain structure evolution in Aluminium cold spray by Monte Carlo method

Pengfei Yu, Shuo Yin, Rocco Lupoi

Trinity College Dublin, The University of Dublin, Department of Mechanical, Manufacturing & Biomedical Engineering, Parsons Building, Dublin 2, Ireland

Abstract

Cold spray (CS), a solid-state depositing technique, has recently demonstrated promising application in additive manufacture (AM). Compared with fusion based AM technique, cold spray can eliminate solidification defects and is appropriate to fabricate some materials that are difficult for high energy beam methods, such as Aluminium. In the cold spray process, extreme plastic deformation will occur, which triggers the severe dynamic recrystallization and result in the formation of ultrafine grain structure. For a dense CSed component, the grain structure highly influences its performance. Especially for the grain structure in the region around the impact interface, which decides the bonding of particles. However, due to the extreme processing condition of CS and complicated deformation history around the interface, it is challenging to carryout systematic study on the factors that influence the finial grain structure and make a prediction on the final grain size in this region. Here, a Monte Carlo model was built to simulate the dynamic recrystallization in the Aluminium cold spray process. The influence of impact velocity and single/multiparticle impact on the final grain structure in the interface was investigated comprehensively and independently. And the average grain size on the impact interface predicted by the modelling agreed well with reported experimental results

Introduction

Cold spray (CS) is a kind of deposit method that powder particles are accelerated to a high velocity by heated high pressure gas traversing through De-Laval nozzle and impact on the substrate to create deposit (Ref 1). In comparison to the thermal spray technique, the bonding between the power particle is achieved by the mechanical interlocking and metallurgical bonding due to the occurrence of severe plastic deformation in the impact process(Ref 2). The solid-state bonding process makes CS as a perfect technique to create aluminium coatings. In recent year, CS has also been treated as an additive manufacture technique to fabricate or repair Al components (Ref 3). Despite all the advantages that CS has in the aluminium depositing, it cannot be neglected that the mechanical properties of CSed Al component cannot match its casting or forging counterpart. Therefore, great effort has been taken in the community to investigate the factors that affect the properties of CSed Al deposit (Ref 4–6). In addition to large scale defects like porosity and unbonded interface, the microstructure of deposit can strongly influence the properties (Ref 1).

Although it is widely accepted that CS can retain the majority of microstructure in the powder particles into deposit, the severe deformation in the impact process will result in a higher dislocation density, amorphization, twinning and formation of ultrafine grain structure via dynamic recrystallization (DRX) (Ref 7–12). Among them, ultrafine grain structure always occurs in the region close to the impact interface due the severest deformation condition in this region and grains as smaller as 10 nm could be formed after the CS process (Ref 12). For a high quality CSed deposit, the occurrence of ultrafine grain structures is crucial for the improvement of strength and hardness. Although experimental investigation has been widely conducted to find out the factors that influence the evolution of grain structure after the CS, because processing parameters including gas pressure, temperature can affect the deformation condition by affecting impact velocity of the particle and it is difficult to separately investigation the influence of CS parameter on grain structure. Moreover, due the extreme short time scale (tens of nanoseconds) and small scale of the impact particles it is impossible to conduct in-situ observation on grain structure evolution process.

In contrast to experimental method, numerical simulation can overcome all the limitations in experimental method and can be used to investigate the factors that influence the final grain structure separately. Up to

now, various numerical simulation studies has been carried out to studies the microstructure evolution during the CS process and different modelling techniques has been taken (Ref 6,13–17). Among them, due the small size scale and short time scale of particle impact process, molecular dynamics (MD) simulation has been widely taken to achieve the grain structure simulation in CS. By using this method, the occurrence of twinning, amorphization and dynamic recrystallization has been successfully modelled and predicted in different materials (Ref 14,15,17). Moreover, it has been found that the grain structure and crystalline orientation of powder particle can influence the deformation behaviour in the impact process (Ref 13). However, despite all the prediction and finding has been made by MD method, it should not be ignored that limited by the huge computing cost of MD methods, it is difficult to conduct large size and long time period MD simulation with a short CPU time. As the consequence of that, up to now the majority size of MD simulation region is about tens of nanometers but the normal average size of powder particle used in the CS is about 35 μm. Wang et al. has used an analytical grain refinement model accompanied with a modified FEA model to investigate investigated grain refinement process during the CS Cu particles (Ref 6). But the analytical model cannot reflect the real physical process of dynamic recrystallization.

In addition to the MD simulation and analytical prediction, other numerical simulation, including phase field (PF), cellular automaton (CA) and Monte Carlo (MC) methods, have been applied to analyse the changes of microstructure in different severe plastic deformation condition. Among them, Monte Carlo method based on the probability and statistics theory do not has limitations in size time scale and has been used to model the dynamic recrystallization process in various deformation conditions (Ref 18,19). Recently, owing to the great improvement of computer performance, the efficiency of Monte Carlo simulation became relatively high. In this work, a Monte Carlo DRX model was used to simulate the grain structure in the region close to impact interface in the Al cold spray process. The model was validated with previous experimental studies. The influence of impact velocity on the grain structure was investigated. Finally, the grain structure formed in single and multiparticle impact condition was modelled and the factor resulting in the variation of grain structure was analysed in detail.

Mathematical modelling

General description of the model

It is known that in the deformation process, the grain structure evolution process is decided by the thermal-mechanical history in the deformation. The variation of thermal-mechanical history actually reflects the conversion of mechanical energy that is input to the materials via different processing methods. In a deformation process, mechanical energy was converted into thermal and strain energy. The increase of thermal energy leads to the increase of temperature. The strain energy stored in materials via the multiplication of crystalline defects, majorly in dislocations, and is known as stored energy. The increase of stored energy results in the increase of flow stress during the deformation makes the deformed material became thermodynamic instable. Once temperature rise to a specific value, dynamic recovery and dynamic recrystallization will occur to dissipated redundant stored energy and bring the deformed material back to a thermodynamic stable status. Because of the dissipation of redundant stored energy, flow stress gradually decreases to a saturate value σ_{sat}, and finer DRX grain structures having less defects formed. After the formation of finer DRX grains, the grain boundaries area increases incredibly, which indicated that the majority of the redundant stored energy has converted to the grain boundaries energy.

In general, the DRX process in the deformation can be treated as an energy conversion process that the mechanical energy is partially converted into the stored energy that is mostly saved in dislocations, and then into grain boundary energy by dynamic recovery and DRX, in which dislocations will react to each other and form finer DRX grains or subgrain structures. Although various DRX mechanisms have reported, the energy conversion pathway is unchangeable. According to this scenario, a model based on the nucleation and growth of new-born DRX grains and minimum stored energy principle was built by author to simulate the grain structure evolution process. It should be noted that phenomenologically among three major DRX mechanisms, DRX formed by CDRX and GDRX do not have clear nucleation and growth stage but more rely on the continuous geometrical changes on lattice(Ref 20,21). Especially for the GDRX, severe elongation and compression of grain will occur in this mechanism (Ref 22,23). However, limited by the ability of present Monte Carlo methods, the geometrical effect on the grain structure was not considered in the present model.

Fig. 1 demonstrates the procedure of the Monte Carlo DRX model based on the energy transformation pathway in the deformation. It consists of three parts, i.e., the stored energy increment, the nucleation and the DRX grain growth. With the increasing of strain in metals, the stored energy U gradually increase. When the value of U exceeds that of U_{sat} (the stored energy corresponding to the saturated flow stress σ_{sat}), the nucleation happens, and the redundant stored energy Un is dissipated. After the nucleation, if the remnant stored energy U_2 is still higher than U_{sat}, the newly formed nucleus with low stored energy will continuously grow up and a part of the stored energy (U_g) will be continuously dissipated until the remnant energy U_3 becomes lower than U_{sat}. Then, the DRX process stops. If the stored energy in the grain exceeds the U_{sat} again, a second run of DRX process will occur on it. This process will keep repeating until the deformation comes to an end.

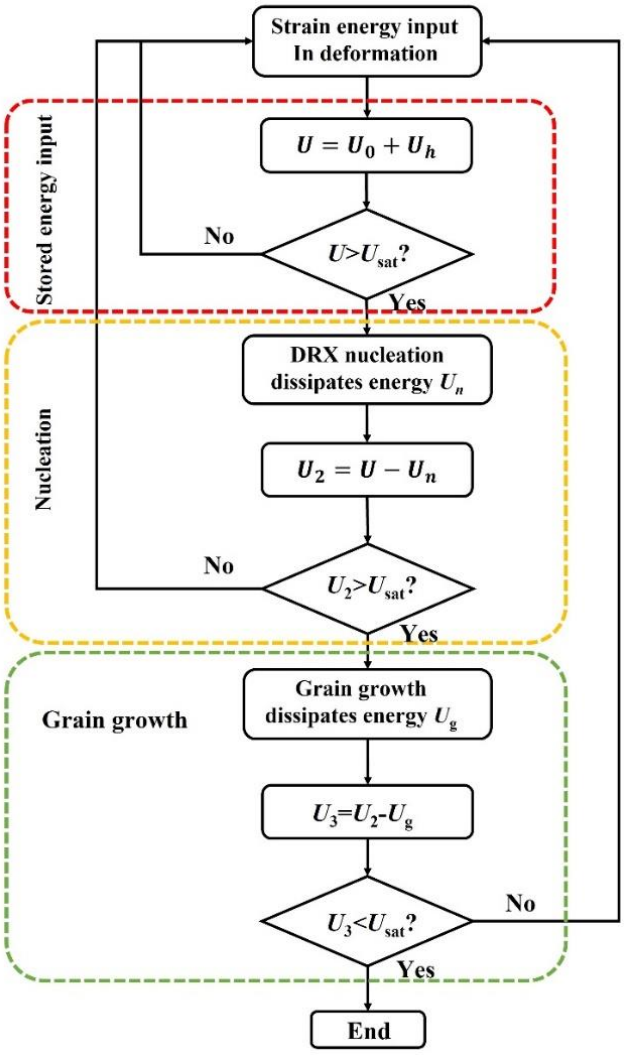

Fig.1 Monte Carlo simulation procedure

Although the ignorance of geometrical effect results in some limitation in its application, the influence of geometrical effect on the grain structure is only striking in the intermediate stage of DRX. For the grain structure produced after completely finished DRX process, factors deciding the DRX grain structure are strain rate and deformation temperature. Therefore, herein, the developed model is plausible to achieve the grain structure simulation and predication in the situation in which DRX process is completely finished.

For example, the developed model here has been successfully applied to model the grain structure evolution process in the welding nugget zone during the friction stir welding (Ref 24).

Stored energy variation

The stored energy is the important driving force of DRX. To develop a reasonable DRX model, it is necessary to establish an appropriate sub model of stored energy. Dislocations, as a kind of crystal defects, play a crucial role in metal plastic deformation, which are also the media between the stored energy and microstructure. The stored energy H_{dis} in per dislocation is expressed as (Ref 25) :

$$H_{dis} = aGb \tag{1}$$

Where a is a constant describing the type of dislocation, G is the shear module and b is the magnitude of the Burgers vector.

When the flow stress becomes saturated, the dislocation density corresponding to σ_{sat} is expressed as ρ_{sat}, and both have following relation(Ref 26,27):

$$\sigma_{sat} = MGb\sqrt{\rho_{sat}} \tag{2}$$

where M is the averaged Taylor factor. The dislocation density caused by work-hardening is represented by ρ_h, and the dislocation density consumed by dynamic recrystallization is represented by ρ_s. Both have following relation according to Kocks-Mecking model (Ref 28):

$$\frac{d\rho_{sat}}{d\varepsilon} = \frac{d\rho_h}{d\varepsilon} + \frac{d\rho_s}{d\varepsilon} \tag{3}$$

where ε is the strain. The first term on the right-hand side of Eq. (3) is the augment of dislocation density due to work-hardening, which is written as:

$$\frac{d\rho_h}{d\varepsilon} = k_1\sqrt{\rho_0} \tag{4}$$

ρ_0 is the initial density of dislocations and the coefficients k_1 is calculated by:

$$k_1 = \left(\frac{G}{G_0}\right)\frac{1}{100Mb} \tag{5}$$

Where G_0 is the constant for unit unification. Considering the variation of strain with time, Eq. (3) can be manipulated as:

$$\frac{d\rho_h}{dt} = k_1\sqrt{\rho_0}\frac{d\varepsilon}{dt} \tag{6}$$

were, $d\varepsilon / dt = \dot{\varepsilon}$ is equal to the strain rate. Consequently, the energy stored in work-harden process, U_h, is described via the combination of Eq. (1) and Eq. (6),

$$\frac{dU_h}{dt} = H_{dis}k_1\sqrt{\rho_0}d\dot{\varepsilon} \tag{7}$$

Based on Eq. (1) and Eq. (2), the stored energy Usat corresponding to the saturated flow stress σ_{sat} for a 2D system with area of S can be expressed as:

$$U_{sat} = \frac{a}{Gb}\left(\frac{\sigma_{sat}}{M}\right)^2 S \tag{8}$$

Here, U_{sat} is used as the criterion to decide the initiation and ending of DRX.

Nucleation model

For DRX, different from that in liquid state, atoms in solid state are tightly constrained. In fact, the driving force of DRX is the stored energy in work-hardened grains and the generation of DRX grains depends on the evolution of crystal defects such as voids and defects. Here, a more practical nucleation model is proposed based on evolution of stored energy and substructures. The nucleation rate model is used to determine the initial nucleation numbers $\dot{N}_0$ and the nucleation possibility P_n. The nucleation rate is the multiplication between $\dot{N}_0$ and P_n. The procedures involved in deciding final nucleation rate are given as follows:

If the total stored energy U in the system exceeds the U_{sat}, then the nucleation process is induced. According to the difference of stored energy between U and U_{sat}, the initial amount of nucleus is expressed as:

$$\dot{N}_0 = \frac{U - U_{sat}}{9\bar{E}_s} \tag{9}$$

Where $\dot{N}_0$ the initial amount of nucleus is, $\bar{E}_s$ is the average stored energy of the elements in the system. In this model, each nucleus consists of 9 elements and the stored energy in these elements is zero. Once the nucleation is successful, the original elements with higher stored energy will be replaced by nucleus elements. Then, the stored energy will be partially consumed.

After the initial nucleus number is determined, the nucleation position is chosen randomly in modelling region. As stated above, nucleation will only locate at grain boundary. Once the position is chosen whether the position is at grain boundary will be judged. If not, another position will be found until the nucleation position is located at grain boundary.

However, whether nucleation at grain boundary is successful is still dependent on the nucleation possibility. When the energy stored in grains is enough to overcome the grain boundary energy, the subgrains boundary will migrate, and the subgrains which reach the critical radius of nucleation will make DRX happen (Ref 29). The critical radius of subgrains r_c is written as follows:

$$r_c(t) = \frac{2\gamma}{U_G(t)} \tag{10}$$

where γ is the grain boundary energy, and U_G is the stored energy in a grain, which varies with time t. Therefore, if the radius of subgrains r_{sub} in the grain boundary is bigger than r_c, the DRX nucleation will happen. Hence, in order to make sure whether the DRX nucleation can occur, it is necessary to know the subgrains size distribution and variation in a grain.

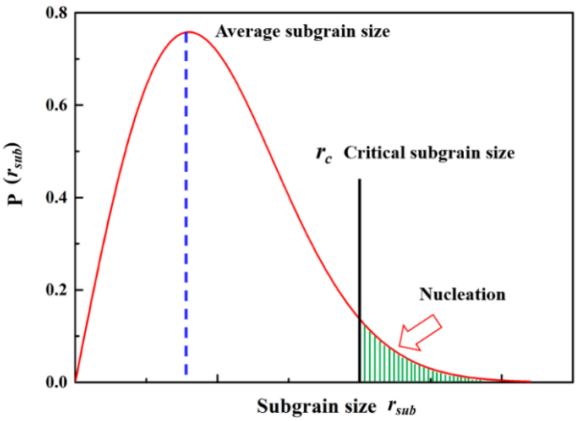

Fig. 2 Rayleigh distribution of subgrains size in a grain

It has been found that the distribution of subgrains size in a grain presents the features of Rayleigh distribution, as shown in Fig. 4. The probability density function is expressed as follow(Ref 30,31):

$$f(\chi) = \frac{\pi}{2}\chi^2 \exp\left(-\frac{\pi}{4}\chi^2\right) \tag{11}$$

where $\chi = r_{sub} / \bar{r}_{sub}$, r_{sub} is the subgrain radius, and $\bar{r}_{sub}$ is the average radius of subgrains. Some experiment evidences have proved that in deformation, the average subgrain size has special relation with Zener-Holloman parameter Z, which is expressed as(Ref 32):

$$\bar{r}_{sub} = \frac{1}{2}(A_1 - B\log Z) \tag{12}$$

Where A_1 and *B* are constants, and Z is written as:

$$Z = \dot{\varepsilon}\exp\left(\frac{Q_s}{RT}\right) \tag{13}$$

Where Qs is the active energy of deformation, R is the gas constant and T is absolute temperature.

As shown in Fig. 4, in the area of the shadow region those subgrains with such radius can become the nucleus of DRX and the probability P_n. For Eq.11, the nucleation probability is the integration of probability density function $f(\chi)$ within $(\chi_c = r_c / \bar{r}_{sub}, +\infty)$, which is written as:

$$P_n = \int_{\chi_c}^{+\infty} f(\chi) d\chi = \exp\left(-\frac{\pi\chi_c^2}{4}\right) \tag{12}$$

Combining the initial nucleation amount $\dot{N}_0$ with P_n, the final nucleation rate is expressed as:

$$\dot{N} = \dot{N}_0 \exp\left(-\frac{\pi\chi_c^2}{4}\right) \tag{13}$$

Grain growth model

After the completion of nucleation process, most part of stored energy input by work hardening is consumed. If there are still extra stored energy that makes the total energy higher than U_{sat}, the new-born DRX nucleus and the grains with low energy will grow up to run out of the extra energy. In this work, the grains growth is stimulated via Monte Carlo Q-Potts model(Ref 18,33–35). Here, only some vital steps are demonstrated.

The size of modelling region is 1000×1000 nm around the tracking point. At the beginning, the modelling region is dispersed as grids, and each point of grids is assigned a random orientation number ranging from 1 to Q, where Q is the maximum value of grain orientation number. The adjacent points with same orientation number are considered as a single grain, while the region where the adjacent points with different orientation numbers is defined as grain boundary. The grain boundary energy is defined as an interaction between nearest neighbour lattice sites(Ref 18). The local interaction energy, E_i, is expressed as,

$$E_i = J\sum_{i,j}^{n}\left(1-\delta_{Q_iQ_j}\right) \tag{14}$$

where J is a positive constant which sets the scale of the grain boundary energy, δ is Kronecker's delta function, Q_i is the orientation at a randomly selected site i, Q_j are the orientations of its nearest neighbours, and n is the total number of the nearest neighbour sites. The value of δ will be set as zero if the nearest neighbours have unlike orientation. Otherwise, the δ will be equal to one. Furthermore, for DRX modelling, the effects of stored energy should also be taken into account and Eq. (14) can be written as (Ref 36):

$$E_i = J\sum_{i,j}\left(1-\delta_{Q_iQ_j}\right)+E_{s,i} \tag{15}$$

where $E_{s,i}$ is the stored energy of site i.

To simulate grain boundary migration, a site is randomly selected, its orientation is changed to one of its nearest neighbour orientations, and the energy variation resulted from the attempted orientation change is calculated. This reorientation is accepted with a probability, which is given as (Ref 35) :

$$p_1 = \begin{cases} 1, & \Delta E \le 0 \\ \exp\left(-\dfrac{\Delta E}{k_B T}\right), & \Delta E > 0 \end{cases} \tag{16}$$

where ΔE is the energy variation due to the change of orientation, k_B is the Boltzman constant, and T is the temperature. Thus, any successful reorientation of a grain to orientations of nearest neighbour grains corresponds to boundary migration. When all the sites in a system have been selected for orientation change, a step of Monte Carlo simulation has been completed.

In order to achieve the grain growth stimulation, it is crucial to obtain the temperature-time history. However, the Monte Carlo stimulation time step (MCS) does not have direct relation with the real time t. Therefore, the relation between the MCS and time t should be established. Here, the grain boundary migration method (Ref 19) has been used to correlate MCS with time t. The expression of the MCS can be written as:

$$(\mathrm{MCS})^{2n_1} = \left(\frac{D_0}{K_1\lambda_0}\right)^2 + \frac{4\gamma A Z_a V_m^2}{N_a^2 h K_1^2 \lambda_0^2}\exp\left(\frac{\Delta S_f}{R}\right)\exp\left(-\frac{Q_a}{RT}\right)t \tag{17}$$

where D_0 is the initial average grain size,λ_0 is the grid spacing, K_1 and n_1 are model constants, γ is the grain boundary energy, A is the accommodation probability, Z_a is the average number of atoms per unit area at the grain boundary, V_m is the atomic molar volume, N_a is Avagadro's number, h is Planck's constant, ΔSf is the activation entropy, Q_a is the activation enthalpy for grain growth, T is the absolute temperature, R is the gas constant, and t is the real time.

Results and discussion

Fig.3 shows the starting grain structure of pure aluminium for Monte Carlo simulation, which is obtained by the Monte Carlo grain growth simulation that did not have nucleation process. The obtained starting grain structure has an average grain size of 1.25μm, which has the same grain size scale with aluminium powder used in the practical CS process. It should be not that because the deformation is severest in the region close to impact interface, which also induce complicated grain structure in this region. Moreover, grain structure here also plays an important role in the bonding mechanism of particles and strongly affects the mechanical properties of the CS deposit. Therefore, this work focus on the modelling and prediction of grain structure in the region close to impact interface. And the position where the Monte Carlo microstructure

simulation was conducted is demonstrated on the left of Fig.4a. the position is located within 1 μm from the impact interface and is 45° from the southern pole of the particle.

Verification of the developed Monte Carlo model

Before the discussion, to verify the feasibility and accuracy of the developed Monte Carlo model and algorithm in the application of CS process, herein, the simulated grain structure was compared with the grain structure obtained by the experimental investigation reported by Liu et al (Ref 12). In their work, spherical pure aluminium powder with average diameter 36 μm were deposit on the substrate. The temperature of gas propelling gas is 523 K and the measured velocity of the aluminium particle is 665m/s. these parameter was used to simulate the impact process via FEA analysis. The deformation parameter, including strain rate and deformation temperature was taken and input to the Monte Carlo simulation program.

To make the simulation close to the practical impact process, a 1/4 3D multiparticle impact process FEA analysis was conducted. The right image on the left of Fig.4a demonstrates the FEA analysis result after the impact process. It can be seen that the first impact particle was severe deformed and jetting structure formed along periphery of the particle. Fig. 4c and Fig 4b show the Monte Carlo simulated grain structure and the histogram of grain size of simulation results. Due to the severe plastic deformation in the impact process, the grain structure has strongly refined to smaller equiaxial grains due to the completely finished DRX process. The average grain size was 33nm and grain with size ~10 nm also formed after the extreme high strain rate deformation. The average grain size obtained by MC modelling is similar to the average grain size measured by Liu et al via TEM characterization and it is also in the same scale of average grain (50~100nm) reported by other experimental investigations (Ref 5,37,38). Consequently, it is plausible to infer that the developed model is also valid in the simulation and prediction of grain structure evolution in the application of cold spray. But it should be noted again that the accuracy is striking, only when the DRX process in the modelling zone is completely finished. The small difference between the simulation and experimental measurement proves that the extension of DRX was extreme high in the region close to the impact interface.

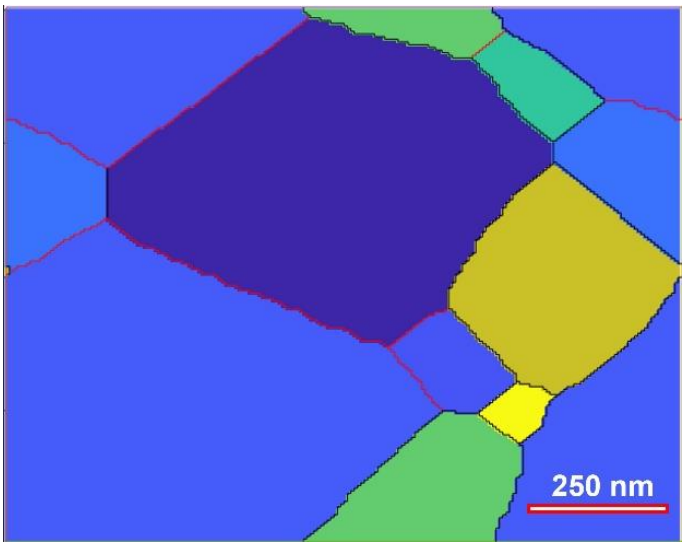

Fig.3 starting grain structure in the modelling

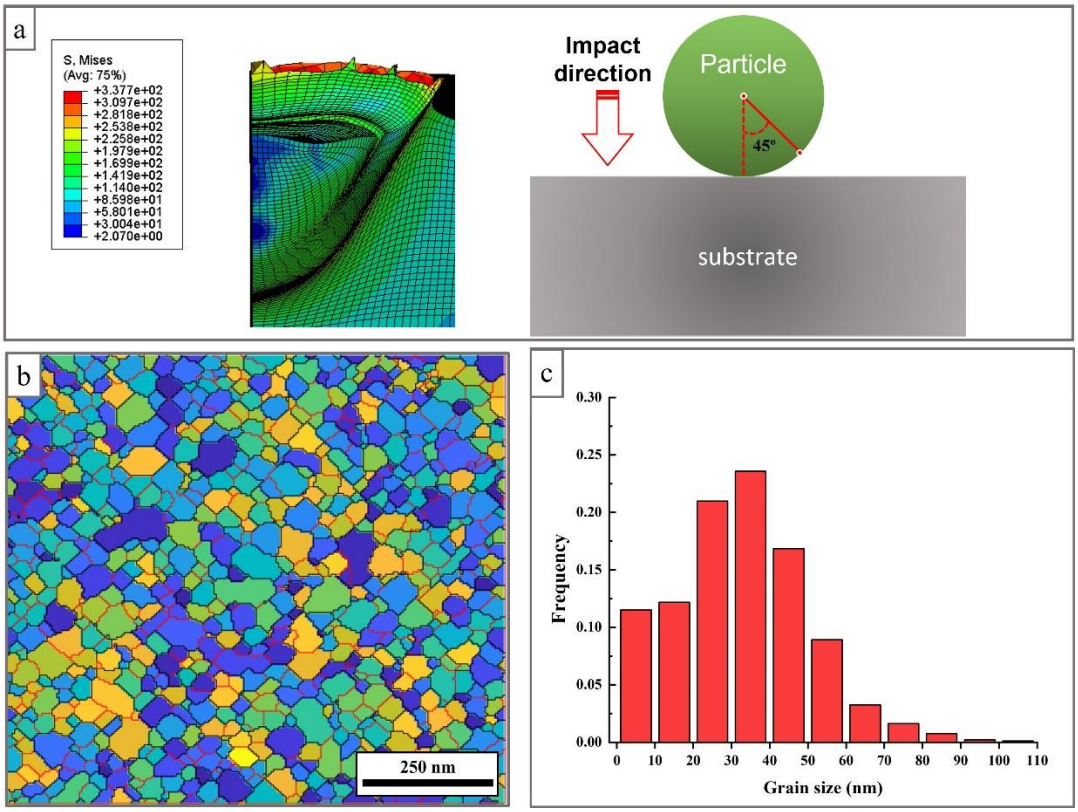

Fig.4 verification of simulated grain structure (a) multiparticle impact process modelled by FEA and the scheme of grain structure modelling position. (c) grain structure obtained by MC modelling and (b) histogram of grain size obtained by MC modelling.

Particle velocity influence on the grain structure

Velocity that was directly influence by gas parameters is an essential factor that decides the deformation condition in the CS and consequently influence the success of bonding of particles. To investigate the influence of impact velocity on the final grain structure, a series of impact velocities were token to simulate the variation of grain structure and studied the influence of impact velocity. In the simulation, the temperature was set as 523 K. Fig.5a shows the simulated grain structure after impact with different velocity and the average grain size is demonstrated in Fig.5b. it can be seen that in the range from 400 m/s to 500 m/s, grains became finer with increase of impact velocity. However, when the impact velocity increased to 600 m/s, grain was larger than that in 400m/s and 600 m/s. it is interesting that with continuous increase of impact velocity after the velocity reached 600 m/s, grains gradually became smaller. But at the velocity of 800 m/s, although the grain was much smaller than 600m/s, abnormal growth of grains (highlighted in the white circle) occurred.

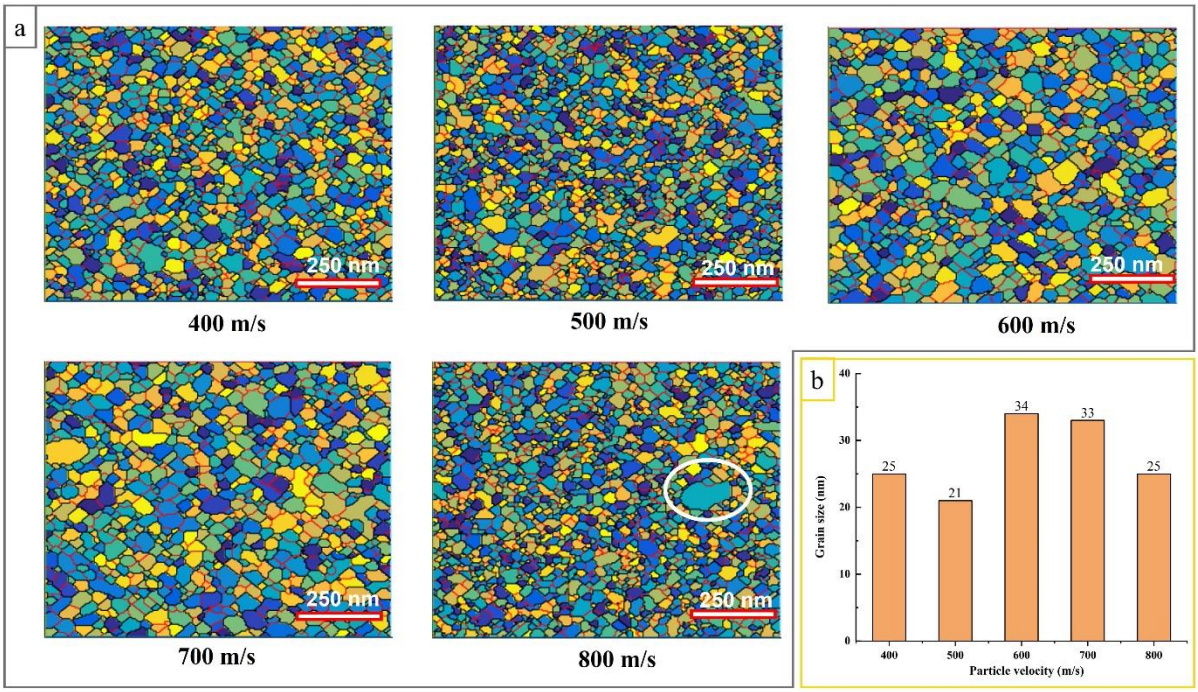

Fig.5 (a) the simulated grain structure in different impact velocity and (b) the variation of average grain size.

As introduced above, deformation parameter decides the grain structure formation in a deformation process. Thus, the variation of strain rate and deformation temperature was extracted and their maximum value in different impact velocity were demonstrated in the Fig.6a. it can be seen that the strain rate and deformation temperature increase with impact velocity becoming higher. higher strain rate result in a larger increment of stored energy in unit time. Thus, in order to dissipate larger stored energy, nucleation rate was higher and grain size was consequently smaller. Due to the activation of atomic migration at higher temperature, grain boundaries can migrate faster, which induce the growth of grains. Especially for DRX grains, because their low stored energy statues, DRX grains were prone to grow with the assistance of thermal activation to reduce the stored energy in the system to the lowest state. Actually, the influence of strain rate and deformation temperature could interact with each other then decide the flow stress and final grain structure. To present the inaction between the strain rate and deformation temperature, Zener-Holloman parameter (expressed as Eq.13) was taken, which not only reflect the influence of deformation parameter but also take the material properties into consideration. a lower Z value suggests more outstanding strain hardening effect and higher nucleation rate induce by larger strain or lower deformation temperature. The changes of Zener-Holloman in different impact velocity are shown in the Fig.6b. The maximum value of Zener-Holloman variation has same increased tendency with strain rate and temperature, which indicated that compared with strain rate increasing, generally, the influence of temperature is not as outstanding as strain rate. It can be seen in the Fig.6b that the difference of Zener-Holloman parameter among 400 m/s, 500 m/s and 600m/s is small. But there is a relatively large increment of strain rate when the velocity comes to the 500 m/s, which results in a severer nucleation and consequently led to a small grain size. However, in comparison to 500 m/s, the increase of strain rate was less outstanding and thus, a higher deformation temperature promoted the grain growth, which consequently result in a larger grain size at 600 m/s. After 600 m/s, with impact velocity becoming faster, the strain rate increased rapidly at velocity 700 m/s and 800 m/s but the rising of temperature is mild, which also results in the outstanding increase of Zener-Holloman parameter. Due to the higher strain rate, the stored energy was also higher and more DRX grains was formed to dissipate suddenly increased stored energy. As consequence of that, grain structure became smaller. When the velocity came to 800 m/s, strain rate reaches the maximum and smallest grain structure is formed. However, because large amount of stored energy was input, the nucleation of DRX could not dissipated the extra stored energy to the balance status. Therefore, some grains with lowest stored energy grew rapidly, which caused the abnormal growth of grains.

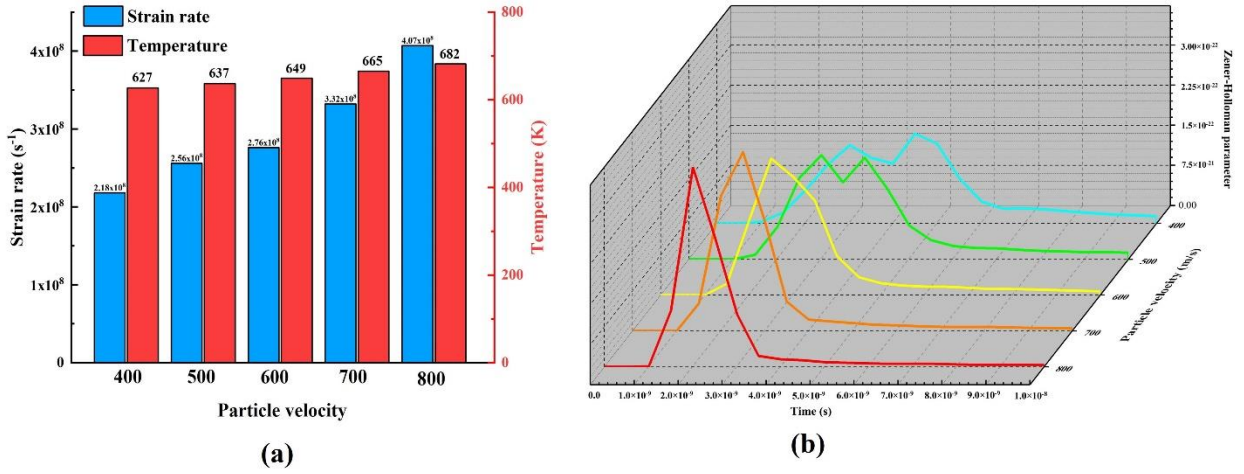

Fig.6 the FEA simulated maximum strain rate, deformation temperature (a) and (b) Zener-Holloman parameters in different impact velocity

Formation of grain structure in single and multiparticle

To investigate the grain structure evolution process in CS process, the characterization on single particle has been widely conducted by taking the advantage of focus ion beam (FIB) technique. But this method cannot represent the real situation in the CS, because the formation of deposit via CS is the consequence of impact and bonding of a large amount of particle. Therefore, the firstly deposited particle will go through a continuous deformation induced by continuous impact of following particles, which influence the final grain structure in the deposit. if the microstructure is taken to study the grain structure evolution in CS process, it will be impossible to separate the influence of deformation occurring in the impact process and following hammering of following impact particles apart. Consequently, to have better understanding on the grain structure evolution process in CS, it is necessary to figure out the influence the multiparticle impact model on the final grain structure.

Herein, impact process of single/multiparticle condition and the grain structure evolution were separately modelled. It should be noted that the simulation zone is chosen from the same position as shown in Fig.4a. The velocity and starting temperature of the particle were 400 m/s and 573K respectively. Fig. 7a and Fig. 7b shows the grain structure obtained by MC modelling in single and multiparticle condition. And Fig.7c and Fig.7d demonstrate the variation of strain rate and deformation temperature for single and multiparticle impact process. It can be seen that grain structure in multiparticle situation is much coarser than that in the single particle condition.

According to the variation of strain rate in two impact condition, there were no obvious difference in the maximum value of strain rate between two conditions, but it was no doubt that the strain rate of multiparticle impact was higher than that in single particle impact. Moreover, as highlighted in the circle of Fig.7c, when the strain rate of single particle came to the zero, due the impact of second particle, the strain rate of multiparticle increased again. But it should be noted that the second turn increase of strain rate was much lower than that in the first impact process. On the contrary to the small diversity in strain rate, as shown in Fig.7d, the difference of thermal history between two impact conditions is striking. it can be seen that for the single particle impact, with deformation going on, deformation increased to the peak value and rapid went down once impact process ended. However, for multiparticle impact condition, due to the impact of the second particle, after the ending of the impact of the first particle, the deformation did not finish immediately, and temperature was still high. Because of lower increase of strain rate but higher temperature, grains were prone to grow, which consequently result in a coarser grain structure in multiparticle impact condition.

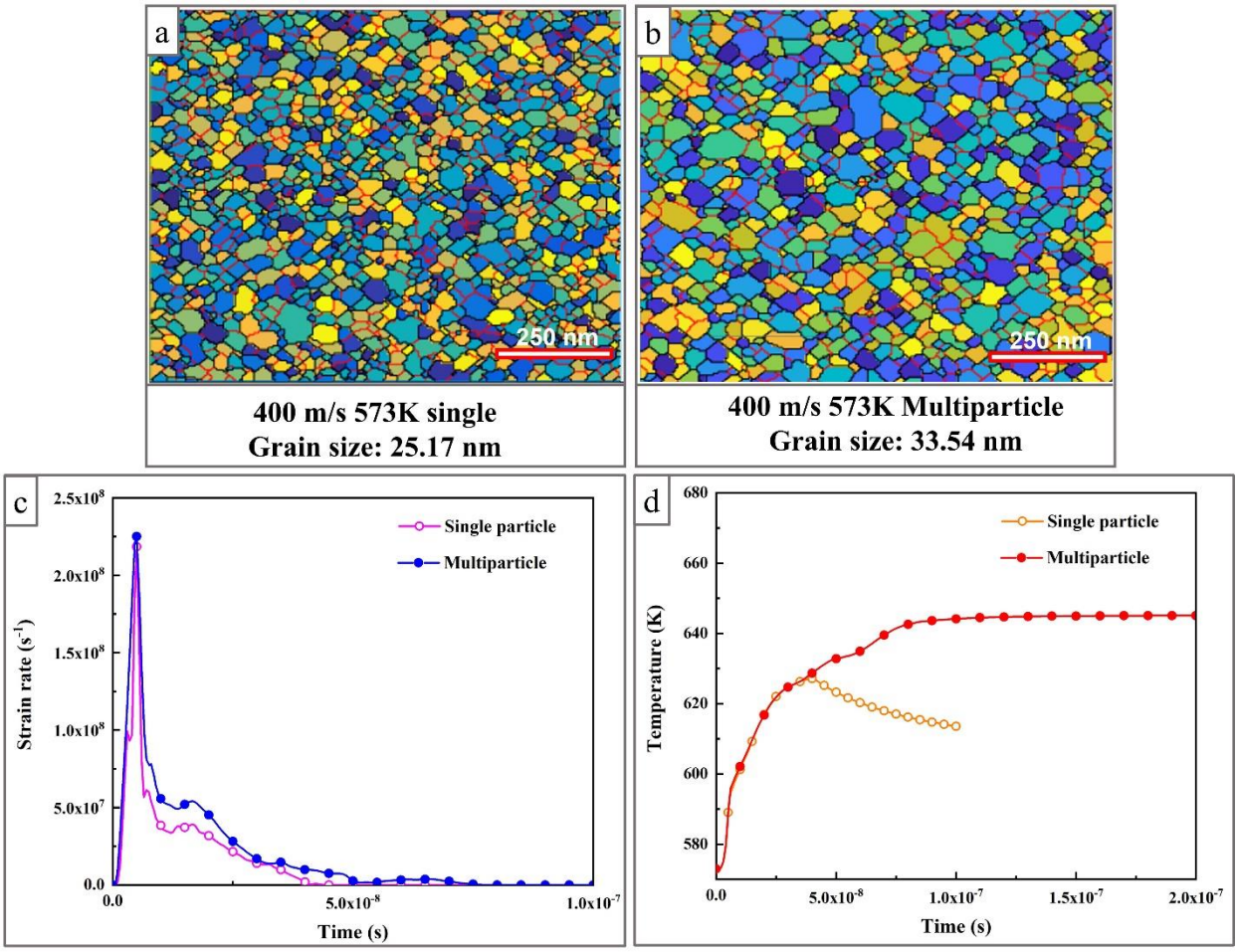

Fig.7 MC simulated grain structure in (a) single and (b) multiparticle impact. FEA calculated the variation of strain rate and deformation during the impact process.

Conclusion

In this work, a developed Monte Carlo DRX simulation model was applied to simulate the formation of grain structures in the region close to the impact interface in the cold spray of Aluminium. The modelling result was used to investigate the influence of particle velocity and single/multiparticle impact on the grain structure. The following conclusions were obtained.

(1) the grain structures in the zone close to the impact interface obtain by Monte Carlo simulation agree well with reported experimental studies. The developed Monte Carlo here is still valid in the application of cold spray.

(2) the influence of impact velocity on grain structure is a complicated process, which is decided by the interaction between the strain rate and deformation temperature. If the higher impact velocity induced more outstanding increase of strain rate than temperature rising, nucleation of DRX grains became the major dissipation pathway for stored energy and finer grain structure was formed. If strain rate did not increase a lot, the higher deformation temperature would let grain growth dominate the dissipation of stored energy and grain structure consequently became larger. However, if the stored energy increased so rapidly that nucleation of DRX could not bring the system back to the lowest stored energy status, grain would grow with an abnormal speed to dissipate the extra energy.

(3) in the multiparticle the increase of strain rate induced by impact is not apparent, which could not result in any difference on final grain structure. On the contrary, due to the input of thermal energy from the impact

of the second particle, a relative high temperature was kept, which resulted in the growth of grain and a coarser grain structure was formed after multiparticle impact.

Reference

1. H. Assadi, H. Kreye, F. Gärtner, and T. Klassen, Cold Spraying–A Materials Perspective, *Acta Mater.*, Elsevier, 2016, **116**, p 382–407.
2. H. Assadi, F. Gärtner, T. Stoltenhoff, and H. Kreye, Bonding Mechanism in Cold Gas Spraying, *Acta Mater.*, 2003, **51**(15), p 4379–4394.
3. W. Li, K. Yang, S. Yin, X. Yang, Y. Xu, and R. Lupoi, Solid-State Additive Manufacturing and Repairing by Cold Spraying: A Review, *J. Mater. Sci. Technol.*, Elsevier, 2018, **34**(3), p 440–457.
4. K.H. Ko, J.O. Choi, H. Lee, Y.K. Seo, S.P. Jung, and S.S. Yu, Cold Spray Induced Amorphization at the Interface between Fe Coatings and Al Substrate, *Mater. Lett.*, 2015, **149**, p 40–42.
5. L. Ajdelsztajn, J.M. Schoenung, B. Jodoin, and G.E. Kim, Cold Spray Deposition of Nanocrystalline Aluminum Alloys, *Metall. Mater. Trans. A*, 2005, **36**(3), p 657–666.
6. Q. Wang, N. Ma, M. Takahashi, X. Luo, and C. Li, Development of a Material Model for Predicting Extreme Deformation and Grain Refinement during Cold Spraying, *Acta Mater.*, 2020, **199**, p 326–339.
7. H. Koivuluoto, M. Honkanen, and P. Vuoristo, Cold-Sprayed Copper and Tantalum Coatings — Detailed FESEM and TEM Analysis, *Surf. Coatings Technol.*, 2010, **204**(15), p 2353–2361.
8. P.C. King, S.H. Zahiri, and M. Jahedi, Microstructural Refinement within a Cold-Sprayed Copper Particle, *Metall. Mater. Trans. A*, 2009, **40**(9), p 2115–2123.
9. W.-Y. Li, H. Liao, C.-J. Li, G. Li, C. Coddet, and X. Wang, On High Velocity Impact of Micro-Sized Metallic Particles in Cold Spraying, *Appl. Surf. Sci.*, 2006, **253**(5), p 2852–2862.
10. S. Yin, Y. Xie, X. Suo, H. Liao, and X. Wang, “Interfacial Bonding Features of Ni Coating on Al Substrate with Different Surface Pretreatments in Cold Spray,” *Materials Letters*, 2015, p 143–147.
11. C.-J. Li, G.-J. Yang, P.-H. Gao, J. Ma, Y.-Y. Wang, and C.-X. Li, Characterization of Nanostructured WC-Co Deposited by Cold Spraying, *J. Therm. spray Technol.*, 2007, **16**(5), p 1011–1020.
12. Z.Y. Liu, H.Z. Wang, M. Hache, E. Irissou, and Y. Zou, Formation of Refined Grains below 10 Nm in Size and Nanoscale Interlocking in the Particle-Particle Interfacial Regions of Cold Sprayed Pure Aluminum, *Scr. Mater.*, 2020, **177**, p 96–100.
13. S. Rahmati, R.G.A. Veiga, B. Jodoin, and A. Zúñiga, Crystal Orientation and Grain Boundary Effects on Plastic Deformation of FCC Particles under High Velocity Impacts, *Materialia*, Elsevier, 2021, **15**, p 101004.
14. L.M. Pereira, S. Rahmati, A. Zúñiga, B. Jodoin, and R.G.A. Veiga, Atomistic Study of Metallurgical Bonding upon the High Velocity Impact of Fcc Core-Shell Particles, *Comput. Mater. Sci.*, Elsevier, 2021, **186**, p 110045.
15. S. Suresh, S.W. Lee, M. Aindow, H.D. Brody, V.K. Champagne, and A.M. Dongare, Mesoscale Modeling of Jet Initiation Behavior and Microstructural Evolution during Cold Spray Single Particle Impact, *Acta Mater.*, 2020, **182**, p 197–206.
16. Z. Liu, H. Wang, M.J.R. Haché, X. Chu, E. Irissou, and Y. Zou, Prediction of Heterogeneous Microstructural Evolution in Cold Sprayed Copper Coatings Using Local Zener-Hollomon Parameter and Strain, *Acta Mater.*, 2020, **193**, p 191–201.
17. S. Rahmati, A. Zúñiga, B. Jodoin, and R.G.A. Veiga, Deformation of Copper Particles upon Impact: A Molecular Dynamics Study of Cold Spray, *Comput. Mater. Sci.*, Elsevier, 2020, **171**, p 109219.
18. M. Morhac and E. Morhacova, Monte Carlo Simulation Algorithms of Grain Growth in Polycrystalline Materials, *Cryst. Res.*, 2000, **35**(1), p 117–128.

19. J. Gao and R.G. Thompson, Real Time-Temperature Models for Monte Carlo Simulations of Normal Grain Growth, *Acta Mater.*, 1996, **44**(11), p 4565–4570.

20. K. Huang and R.E. Logé, A Review of Dynamic Recrystallization Phenomena in Metallic Materials, *Mater. Des.*, 2016, **111**(dec.5), p 548–574.

21. F.J. Humphreys and M. Hatherly, Chapter 13 - Hot Deformation and Dynamic Restoration, F.J. Humphreys and M.B.T.-R. and R.A.P. (Second E. Hatherly, Eds., (Oxford), Elsevier, 2004, p 415–V.

22. M.E. Kassner and S.R. Barrabes, New Developments in Geometric Dynamic Recrystallization, *Mater. ence Eng. A*, 2005, **410**(Nov), p 152–155.

23. R.K.S.M. Motohashi, Continuous Dynamic Recrystallization in an Al–Li–Mg–Sc Alloy during Equal-Channel Angular Extrusion, *Mater. Sci. Eng. A*, 2005.

24. P. Yu, C. Wu, and L. Shi, Analysis and Characterization of Dynamic Recrystallization and Grain Structure Evolution in Friction Stir Welding of Aluminum Plates, *Acta Mater.*, Elsevier, 2021, **207**, p 116692.

25. E.J. Mittemeijer, The Crystal Imperfection; Lattice Defects BT - Fundamentals of Materials Science: The Microstructure–Property Relationship Using Metals as Model Systems, E.J. Mittemeijer, Ed., (Berlin, Heidelberg), Springer Berlin Heidelberg, 2011, p 201–244.

26. E.I.G.-N. and J.S. and P.E.J. Rivera-Díaz-del-Castillo, Dislocation Annihilation in Plastic Deformation: II. Kocks–Mecking Analysis, *Acta Mater.*, 2012, **60**(6–7), p 2615–2624.

27. L.S. Tóth, Y. Estrin, R. Lapovok, and C. Gu, A Model of Grain Fragmentation Based on Lattice Curvature, *Acta Mater.*, 2010, **58**(5), p 1782–1794.

28. U.F.K. Mecking, Physics and Phenomenology of Strain Hardening: The FCC Case, *Prog. Mater. Sci.*, 2003, **48**(3), p 171–273.

29. J.E. Bailey and P.B. Hirsch, The Recrystallization Process in Some Polycrystalline Metals, *Proc. R. Soc. London. Ser. A. Math. Phys. Sci.*, (6 CARLTON HOUSE TERRACE, LONDON SW1Y 5AG, ENGLAND), ROYAL SOC LONDON, 1962, **267**(1328), p 11–30.

30. E.A. Holm, M.A. Miodownik, and A.D. Rollett, On Abnormal Subgrain Growth and the Origin of Recrystallization Nuclei, *Acta Mater.*, 2003, **51**(9), p 2701–2716.

31. D.G. Cram, H.S. Zurob, Y.J.M. Brechet, and C.R. Hutchinson, Modelling Discontinuous Dynamic Recrystallization Using a Physically Based Model for Nucleation, *Acta Mater.*, 2009, **57**(17), p 5218–5228.

32. T. Furu and E. Nes, Growth Rates of Recrystallized Grains in Highly Deformed Commercial Purity Aluminium, an Experimental and Modelling Study, *Mater. ence Forum*, 1993, **113**–**115**, p 311–316.

33. R.B. Potts, Some Generalized Order-Disorder Transformations, *Math. Proc. Cambridge Philos. Soc.*, 1952, **48**(1), p 106–109.

34. Z. Yang, S. Sista, J.W. Elmer, and T. DebRoy, Three Dimensional Monte Carlo Simulation of Grain Growth during GTA Welding of Titanium, *Acta Mater.*, 2000, **48**(20), p 4813–4825.

35. M.P. Anderson, D.J. Srolovitz, G.S. Grest, and P.S. Sahni, Computer Simulation of Grain Growth—I. Kinetics, *Acta Metall.*, 1984, **32**(5), p 783–791.

36. A.D. Rollett, M.J. Luton, and D.J. Srolovitz, Microstructural Simulation of Dynamic Recrystallization, *Acta Metall. Mater.*, 1992, **40**(1), p 43–55.

37. C. Borchers, F. Gärtner, T. Stoltenhoff, and H. Kreye, Formation of Persistent Dislocation Loops by Ultra-High Strain-Rate Deformation during Cold Spraying, *Acta Mater.*, Elsevier, 2005, **53**(10), p 2991–3000.

38. C. Borchers, F. Gärtner, T. Stoltenhoff, and H. Kreye, Microstructural Bonding Features of Cold Sprayed Face Centered Cubic Metals, *J. Appl. Phys.*, 2004, **96**(8), p 4288–4292.